Effects of Friction Stir Welding on Corrosion Behaviors of AA2024-T4 Aluminum Alloy

Steve Korakan Ales[1], Lei Wang[2a]

[1]*Department of Mechanical Engineering, Auckland University of Technology, Auckland, NZ*
[2]*Department of Electromechanical Engineering, Shenyang Aerospace University, Shenyang, China*

Abstract. In this work, the corrosion behavior of welded joints of AA2024-T4 Al alloy produced by friction stir welding process has been investigated. Tests were performed in an aerated 3.5% NaCl aqueous solution with pH = 7 at 20±2°C. Corrosion rate and corrosion morphology of weld regions were evaluated and compared to those of the parent metal. The microstructure of weld nugget, thermomechanical affected zone, heated affected zone, and parent metal were analyzed using scanning electron microscopy and energy dispersive spectroscopy. It was observed that corrosion initiated at FSW related spots and the sizes of local corrosion increased with time.

1 Introduction

Friction stir welding (FSW) is a solid state joining process patented in 1991 by The Welding Institute (TWI). Being a solid-state process, FSW can be used to weld almost any type of metal, including some previously un-weldable precipitation strengthened 2xxx and 7xxxs Al alloys [1]. Under tensile loading, failure of FS welds most often occur in the area between the heat affected zone (HAZ) and the thermomechanically affected zone (TMAZ), where high temperatures dissolve and coarsen the strengthening precipitates, creating local strength minima during FS [2]. Due to the change in precipitate morphology, this region is also generally susceptible to corrosion [3]. The goal of this research was to identify the corrosion mechanisms on FS Al 2024-T4 Al alloys and on the fatigue behaviors.

Aircraft structures made from high-strength Al alloys exhibit a strong propensity to pitting [4]. Corrosion-fatigue in Al alloys generally involves the formation of pits, their growth, nucleation of cracks from pits, and the eventual propagation of the crack leading to failure. Although pits can initiate from both physical and chemical heterogeneities on the surface, the role of inclusions and second-phase particles in inducing pitting corrosion in aluminum alloys is more common. As the alloys contain numerous such particles, electrochemical reactions are triggered between them and the surrounding matrix [5]. Particle-induced pitting corrosion in aluminum alloys has indeed been observed by scanning and transmission electron microscopic techniques [4]. Pitting corrosion is therefore an issue that continues to cause serious concern in the aircraft industry [6].

[a] Corresponding author: leiwng@sau.edu.cn

The mechanism of pitting corrosion and its impact on fatigue in aircraft aluminum alloys has been widely discussed [7]. Corrosion pits are seen to significantly shorten the fatigue crack initiation, decrease the threshold stress intensity by 50% or more, and lower the fatigue strength by about 40% [8]. The pit growth that causes the fatigue crack to initiate is seen to be controlled by the limiting cathodic current density supported by the exposed constituent particles within a growing pit [9].

2 Experimental procedures

There were three steps in conducting the experiments. The first step was to carry out FSW. This was done using a FSW 3LM-4012 machine that uses a tapered needle right hand thread rotation. The diameter of tool was 15 mm, pin diameter was 4.5 mm, length of the pin was 3.7 mm. Tool was made using H13 tool steel. Tilt angle of the tool during FSW was 2°. Tool rotation speed was 1000 rpm and the welding speed was 100 mm/min. The test material used was a 40 mm × 25 mm × 4 mm thick aerospace 2024-T4 Al alloy plate. The chemical composition by mass fraction and mechanical properties are shown in Table 1 and Table 2, respectively.

Table 1 Chemical Composition of Al2024-T4 (wt%)

Al	Cu	Mg	Mn	Si	Fe	Others
91.1	4.4	1.5	1.5	0.5	0.5	0.5

Table 2 Mechanical properties of Al2024-T4 Aluminum Alloy

Tensile strength, MPa	0.2% proof strength, MPa	Elongation, %
420	260	15

Weld burrs along the seam are removed before cutting the samples into 40mm x 25mm x 4mm for testing according to ASTM G31-72 standard for Immersion Corrosion Test for welds. Samples were then submerged in deionized water in a 3.5% NaCl solution (simulated marine environment). The pH value was at 7 and tests were conducted at room temperature (20±2°C). Immersion times were 24, 48, 72, 120, 240 and 480 hours respectively. For 240 and 480 hour immersion, the etchant was replaced after every seven days. For each set of test, two parallel specimens were used for each time. After each test, corrosion products were removed using dilute nitric acid and cleaned using an ultrasonic vibration cleaning equipment. This was followed by static measurement of weight loss due to corrosion rate as defined in equation (1) using a simple weighing balance. Static weight loss method was used to weigh the weight loss of the specimens after corrosion. Equation (1) in the following is used to calculate the corrosion rate (CR):

$$\mathbf{CR}\left(\frac{g}{m^2.h}\right) = 1.0x10^4\, x\, W/(A\, x\, T) \tag{1}$$

where W is the weight loss，A is corrosion area, T is corrosion time**.**

Note that the corrosion rate of the weld is calculated herein as the average corrosion rate, and therefore does not reflect the extent of corrosion of a specific specimen. During a test, corrosion normally started by pitting and the number of pits increased fast at the beginning, while a higher rate and more serious form of corrosion developed later. It is necessary to combine the mass loss and the corrosion rate to comprehensively analyze the severity of the specimen under consideration. Therefore, equation (2) defines the percentage material removal as follows:

$$W_L = \left(\frac{(W_B - W_A)}{W_B}\right) x\ 100\% \tag{2}$$

where, W_L is the % weight loss ratio, W_B is the weight before corrosion, W_A is the weight after corrosion

Hardness tests of the FS welds were carried out by using Vickers hardness instrument. Micro-hardness tests are done with an HVS-1000A Vickers hardness tester across the weld section at evenly spacing of 0.25mm near the TMAZ and 0.5mm for the other zones. The weld was observed using Olympus GX51 optical microscope after corrosion. Characteristics of corroded pits macro-morphology photos were taken for each time per sample using an FEI-QUANTA 600 scanning electron microscope (SEM) with its digital camera, combined with EDS analysis of the corrosion products and phases.

3 Results and analysis

3.1 Microhardness and microstructure

A hardness profile is shown in Fig. 1. Clearly, hardness varies significantly at different points from the centre of the weld. The lowest hardness, approximately 92.2 HV, is found in the TMAZ region approximately 4 mm from the plate joint line. Hardness increases toward the Nugget slightly. A higher hardness, approximately 128.8 HV, is found in the nugget. Hardness in the parent material is much higher than the weld zones reaching around 130 HV. The softening in the weld zone is due to annealing in the zone during FSW.

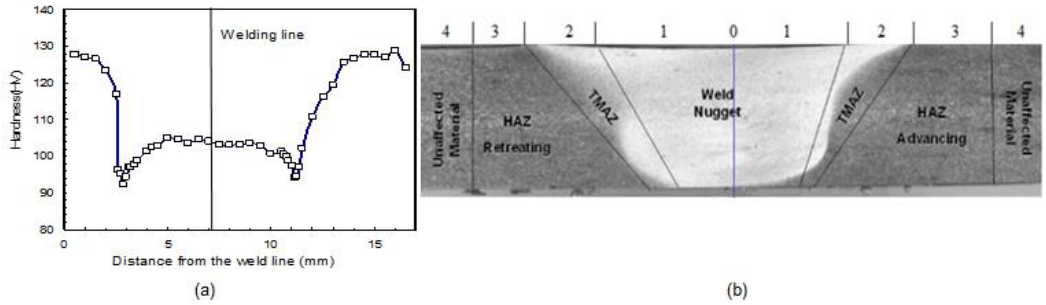

Figure. 1 (a) Vickers hardness transverse across the friction stir welded 2024-T4 aluminum alloy joint at various positions in the section. (b) Different FS Weld Zones affected by weld too during FS welding.

Microstructure in each region of a FSW joint is shown in Fig. 2. The finest microstructure is found in the nugget zone (NZ) which has an equiaxed grains of the order of 5 to 10 μm (Fig.2b). Microstructure present in the TMAZ shows an elongated grain structure that is believed to be due to severe plastic deformation that has taken place during welding, because the stirring action causes the grains of the parent metal to be drawn into and around the nugget zone (Fig.2c). The grain structures in the HAZ and parent plate are similar, with a size of the order of 150 to 200 μm (Fig. 2a and 2d), but we can find more second phase precipitates from the matrix because of the heat from FSW. The variation in grain size in each region depends on the material and process parameters of FSW. The non-uniform microstructure across the FSW joints is believed to introduce different fatigue strength for each zone of the weld.

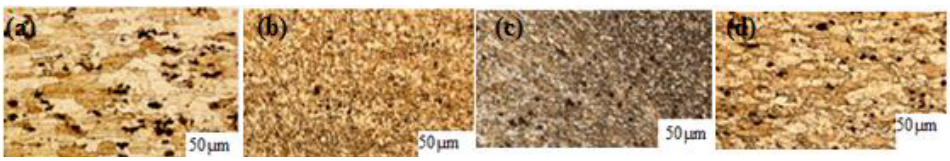

Figure. 2 Microstructures of (a) parent material, (b) nugget (N) region, (c) TMAZ and (d) HAZ.

3.2 Corrosion test results

The following factors may affect the stability of Al oxide and thereby cause corrosion:

- The oxide is not stable in acidic (pH < 4) or alkaline (pH > 9) environments [9]
- Aggressive ions (chlorides, fluorides) may attack the oxide locally.
- Certain elements (Ga, Ti, In, Sn, Pb) may become incorporated in the oxide and destabilize it [10].

Pitting is a highly localized type of corrosion in the presence of aggressive chloride ions. Pits are initiated at weak sites in the oxide by chloride attack [10, 11]. Pits propagate according to the reactions while hydrogen evolution and oxygen reduction are the important reduction processes at the intermetallic cathodes.

As a pit propagates the environment inside the pit (anode) changes. As Al dissolves following reaction (3), according to reaction (4), pH will decrease. To balance the positive charge produced by reaction (3) and (4), chloride ions will migrate into the pit. The resulting HCl formation inside the pit causes accelerated pit propagation. The reduction reaction will cause local alkalinisation around cathodic particles. Al oxide is not stable in such environment, and Al around the particles will dissolve (alkaline pits). The active Al component of the particles will also dissolve selectively, thereby enriching the particle surface with Fe and increasing its cathodic activity. Etching of the Al matrix around the particles may detach the particles from the surface, which may repassivate the alkaline pits. This may also reduce the driving force for the acidic pits causing repassivation of some in the long run.

$$\mathrm{Al} = Al3+ + 3e- \tag{3}$$

$$Al_3^{+} + 3H_2O = \mathrm{Al(OH)_3} + 3\mathrm{H^+} \tag{4}$$

$$2H+ + 2e- = \mathrm{H_2} \tag{5}$$

$$O_2 + 2H_2O + 4e- = 4\mathrm{OH^-} \tag{6}$$

Initial corrosion or pitting corrosion mechanism is based on the second phase dissolution and it started from the weld surface as can be seen in Fig. 3 (a-d) with many small pores and shallow pits. 2024-T4 Al alloy has S phase (Al_2CuMg) and theta phase (Al_2Cu) as the main strengthening phases. Since corrosion potential and matrix phase are similar so that the initial galvanic pitting are established between the S phase and the Al alloy matrix. S phase is about 2.7% of the surface area of the alloy due to its lower corrosion potential, and the preferential dissolution of the anode. When the S phase of the Al, Mg element after dissolution, the remaining elements with a high Cu is electrochemically inert to a large number of enrichment.

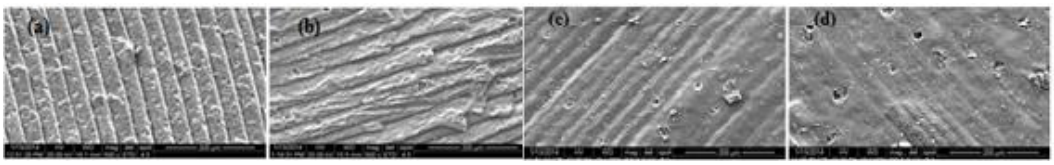

Figure. 3 Pits Morphologies of Weld Surfaces (a) TMAZ, (b) HAZ advancing side, (c) HAZ Retreating side and (d) WN.

Fig. 4 (a, b) shows the surface of the weld at this copper-red color. Enrichment of Cu led to S phase corrosion potential rising above the Al alloy matrix when potential polarity reversal would occur. S phase acted as the cathode and the anode was the dissolving phase meaning corrosion pits, as can be observed in Fig. 4 (a, b, c, d). At this point, Cu element enrichment was the cathode where oxidation reaction took place and the weld surface gradually darkened as shown in Fig. 4 (c, d, and e).

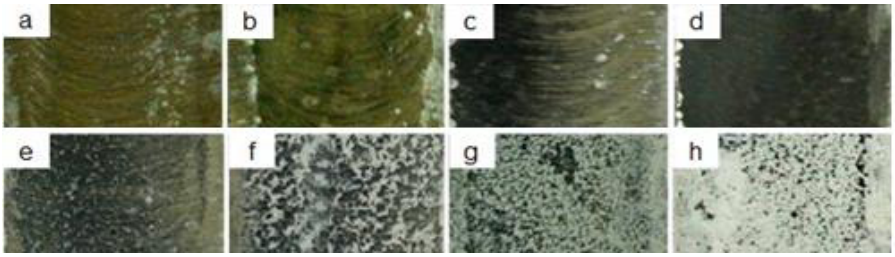

Figure. 4 Macro Morphologies of Corroded FS Weld Surfaces. (a) 24hr (b) 48hr (c) 72hr (d) 96hr (e) 120hr (f) 240hr (g) 360hr (h) 480hr.

With the further development of the corrosion process, the corrosion product began to appear white granular Fig. 4 (e), identified as mainly Al $(OH)_3$ and Al_2O_3, containing a small amount of Mg oxide. When the immersion time was nearly 240 hours, white corrosion particles increased, and further immersion into 480 hours, the weld surface has been covered by a white corrosion product layer, as show in Fig. 4 (f, g, h). Fig. 5 shows pitting at different set of times. The longer the immersion time, the deeper the pit depth. It is obvious that the depth of the pith depends on corrosion time.

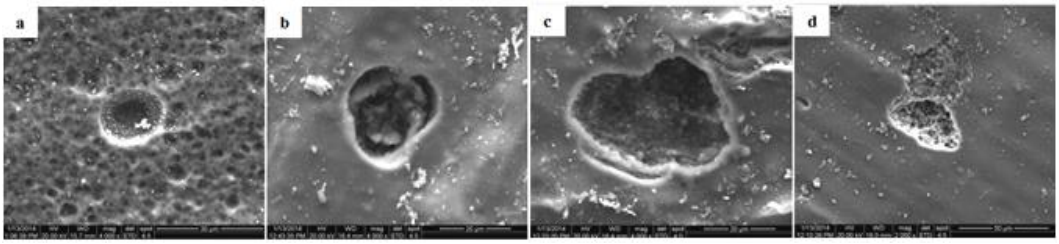

Figure. 5 Morphology of Single Pits. (a) 48h ×4000 (b) 96h ×4000(c) 240h ×4000(d) 480h ×2000.

Decline in Cl^- at the corrosion pit enrichment of pH further promote anodic dissolution in the formation of occluded cell autocatalytic effect. Meanwhile, due to the strengthening phase, mainly in the grain boundaries which appear weak around the Cu precipitation area while there will be a small amount of $MnAl_6$ dispersed in the grain boundaries. This will make the composition of the multiphase system intergranular in the corrosive medium containing Cl^- ions resulting in the occurrence of intergranular corrosion along the grain boundary forming anodic dissolution channels. This stage is mainly due to excessive pitting to intergranular corrosion, where the test piece has less mass loss. Thus corrosion rate is decreased. The spectrum analysis of the weld surface of the elements present in the Cu corrosion after 48 and 480 hours as shown in Fig. 6.

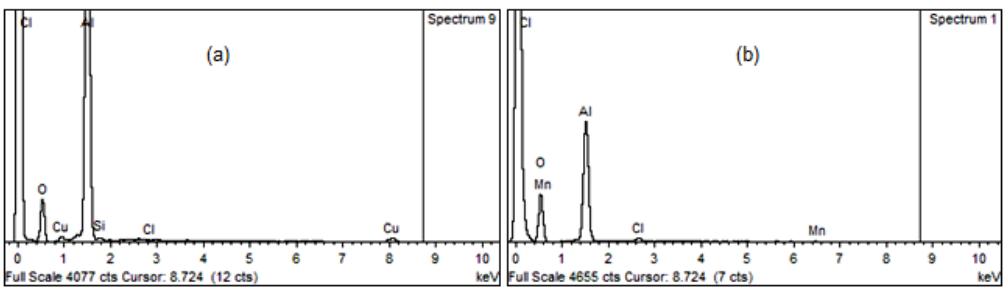

Figure. 6 Results of EDS Analysis (a) Corrosion 48 hr, (b) Corrosion 480 hr,

When immersion proceeded to 480 hours, the development of multiple weld surface corrosion occurred resulting in increased corrosion rate weight loss as shown in Fig. 7 (a, b). Thus, from the

initial weld pitting corrosion develops further denudation, erosion leading to more serious specimen mass loss. Therefore, the corrosion occurs at faster rate.

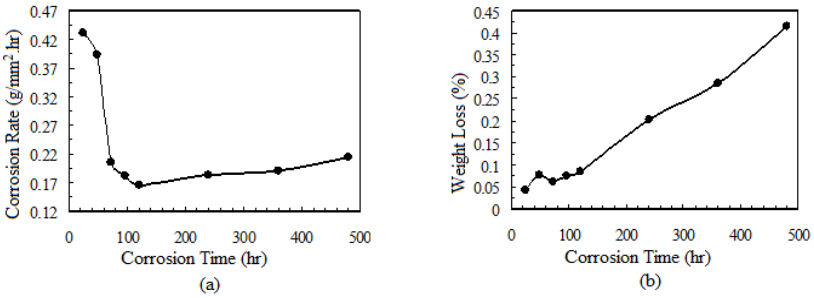

Figure. 7 (a) Corrosion Rate, (b) % weight loss.

4 Conclusions

In age-hardened AA2024-T4 FS weld of thin sheets hardness variations are bigger and are of W-shape with local maximum at weld centre. Variation of hardness (HV) of the FS weld is very lower at the TMAZ region, nugget, HAZ and higher at the parent material.

In FS weld of 2024-T4 aluminium alloy experiences a slow recovery process between the initial transition pitting mechanism and intergranular corrosion.

Due to uneven weld microstructures and precipitate distribution most serious corrosion occurs at weld nugget area, forward side and lighter at the return side.

Pitting in Al-Cu alloys are due to Cu enrichment and redistribution where oxide film breakdown during FS weld which supports anodic reaction.

The longer the immersion time, the more serious is the corrosion of the specimen where corrosion rate increases ultimately due to denudation.

References

1. W.M. Thomas et al. “Friction Stir Welding,” U.S. Patent No. **5,460,317**, October, 24, 1995.
2. Genevois, C. et al., *Acta Materialia*, vol. **53**, no. 8, May, (2005), pp. 2447-2458.
3. Hannour, F. et al. *Proceedings of the 2nd International Friction Stir Welding Symposium*, 26-28 June, 2000.
4. P. L. Threadgill: *Sci. Technol. Weld. Join.*, (2007), **12**, 357-360.
5. A. P. Reynolds, W. D. Lockwood and T. U. Seidel: *Mater. Sci. Forum*, 2000, 331-337, 1719-1724.
6. L. E. Murr, G. Liu and J. C. McClure: *J. Mater. Sci.*, (1998), **33**, 1243-1251.
7. K. A. A. Hassan, P. B. Prangnell, A. F. Norman, D. A. Price and S. W. Williams: *Sci. Technol. Weld. Join.*, 2003, 8, 257-268.
8. Y. K. Yang, H. Dong and S. Kou: *Weld. J.*, 2008, **87**, 202s-211s
9. Davis, J. R. et. al, editor, *Metals Handbook*, volume 13, pages 104-122 and 583-609. Ninth edition, ASM International, Ohio, 1987.
10. Nisancioglu, K., Corrosion of aluminium alloys. *Proceedings of ICAA3*, volume **3**, pages 239-259. Trondheim, (1992). NTH and SINTEF.
11. Scamans, G. M.; Hunter, J. A.; N. J. H. Holroyd. Corrosion of Aluminum - a New Approach, *Proceedings of 8th International Light Metals Congress*, pages 699-705. Leoben-Wien, 1987.